2012 IEEE International Conference on
Multisensor Fusion and Integration for Intelligent Systems (MFI)
September 13-15, 2012. Hamburg, Germany

Outdoor Localization with Optical Navigation Sensor, IMU and GPS

Youngmok Yun, Jingfu Jin, Namhoon Kim, Jeongyeon Yoon, and Changhwan Kim

Abstract— **Autonomous outdoor navigation algorithms are required in various military and industry fields. A stable and robust outdoor localization algorithm is critical to successful outdoor navigation. However, unpredictable external effects and interruption of the GPS signal cause difficulties in outdoor localization. To address this issue, first we devised a new optical navigation sensor that measures a mobile robot's transverse distance without being subjected to external influence. Next, using the optical navigation sensor, a novel localization algorithm is established with Inertial-Measurement-Unit (IMU) and GPS. The algorithm is verified in an urban environment where the GPS signal is frequently interrupted and rough ground surfaces provide serious disturbances.**

I. Introduction

Autonomous navigation algorithm in outdoor environment is an essential part for outdoor robot applications, and diverse studies have been performed in efforts to resolve the outdoor navigation problems [1]. Nevertheless, the maturity level of outdoor navigation algorithms is relatively low compared to that of indoor navigation [2]. One of the main reasons for this is that precise localization of an outdoor mobile robot is more difficult than an indoor environment due to the complex and unpredictable nature of outdoor environments [3] [4].

There are two major causes of serious error in outdoor localization: inaccurate odometry and limitation on the use of Global-Positioning-System (GPS) [5] [6]. First, inaccurate encoder-based odometry causes significant error of outdoor localization. Generally, mobile robot navigation algorithms highly depend on encoder-based odometry as it is the main information used for state prediction [7]. In the case of indoor environment, encoder-based odometry is quite reliable, but in the case of outdoor environment, the odometry is very uncertain due to the unpredictable contact between the mobile robot and ground. Depending on the conditions of the surface, the mobile robot's wheels slip and sometimes rotate in the air [5]. In particular, skid-steering vehicles, which are widely used in research due to their simple structure, suffer from inaccurate motion models and slippage [8].

Y. Yun, J. Jin, N. Kim, J. Yoon are researcher of Korea Institute of Science and Technology, S. Korea

C. Kim is a principal researcher of Korea Institute of Science and Technology, S. Korea , ckim@kist.re.kr

The second problem of outdoor localization is related to GPS. GPS is the most powerful measurement available in outdoor environments because it provides absolute position information. Remark that it is almost impossible to acquire absolute pose information in indoor environments unless artificial landmarks or indoor GPS is exploited. Despite the strong points of GPS, its use is quite limited. The most serious problem is blockage and reflection of the GPS signal from satellites [3]. This interruption of the GPS signal occurs by trees, buildings, and other obstacles, and it presents a crucial limitation to the use of GPS in urban environments.

Numerous researchers have proposed diverse schemes in efforts to solve the aforementioned outdoor problems. In K. Ohno's work [9], the robot identifies its position by encoder-based odometry and (Differential GPS) DGPS. Additionally, Laser-Range-Finder (LRF) was used for 3D feature mapping. S. Panzieri et al [6] suggested an outdoor localization solution using inexpensive commercial GPS and an inertial platform with Kalman filtering. A. Georgiev et al [2] proposed an outdoor localization algorithm particularly for skid-steering vehicles. In their approach, an inertial-navigation-system (INS), magnetic compass, GPS, and encoder-based odometry information were fused. In particular, they tried to calculate an accurate motion model of skid-steering vehicles. Despite the advances realized with the above approaches, large odometry error and obstruction of the GPS signal remain significant issues for outdoor localization.

Against the above problems, first we have developed a new optical navigation sensor that is able to resolve a fundamental problem of encoder-based odometry [10]. The function of the optical navigation sensor is very similar to that of a computer mouse. Because the optical navigation sensor is self-reliant and unaffected by the mobile robot's drift and an inaccurate motion model, its performance for estimating the robot pose is remarkably superior to that of encoder-based odometry.

Our localization algorithm is based on an Extended-Kalman-Filter (EKF). In the prediction step, the robot state is estimated by the optical navigation sensor and an IMU, and then the predicted state is corrected by GPS measurement. In the correction step, DGPS and Single GPS modes are alternatively taken depending on the quality of GPS communication. Additionally, a calibration parameter for the optical navigation sensor is

978-1-4673-2511-0/12/$31.00 ©2012 IEEE

autonomously tuned.

A skid-steering type vehicle is used for the experiment, which was conducted on the campus of Korea Institute of Science and Technology (KIST). The KIST campus is a typical urban environment. Even when the robot moves on rough and rugged ground and passes beside tall buildings that disrupt stable GPS communication, it was able to maintain consistency in estimating its position. The experiment results show that the algorithm tracks the robot's position in an urban environment successfully.

The remainder of this paper is organized as follows. Section II introduces the sensor configuration of the mobile robot system. Section III describes our localization algorithm. Section IV introduces a hardware description and analyzes the experiment results. Finally, our conclusion is given in Section V.

II. SENSOR CONFIGURATION FOR OUTDOOR LOCALIZATION

Before outlining the proposed localization algorithm, we briefly introduce the sensor configuration in this section. The algorithm uses three sensors: An Optical navigation sensor, IMU, and GPS.

A. Optical navigation sensor

The newly developed optical navigation sensor is comprised of an illumination part and a laser mouse sensor. An Avago Technologies ADNS-6010 sensor consists of a 30x30 pixel image sensor and a DSP for image processing. The image sensor in ADNS-6010 takes snapshots of the surface continuously and the DSP extracts features from every image and compares the features to determine the distance and direction traveled and the distance along the x-axis and y-axis. The measured distance information is sent to the host device via RS232 communication.

Since ADNS-6010 is designed for a laser mouse, the sensor functions only when the sensor is 2-3mm above the surface. However, our algorithm aims for outdoor localization, and the sensor should be equipped on outdoor vehicles. We thus used a lens devised for mobile phones. Finally, the image sensor can capture images at 50-60mm from the surface, and is hence applicable for outdoor environments. [10]

The illumination part, which consists of three high power LEDS and a diffuser, helps the image sensor take snapshots in constant lighting conditions. By the aid of the illumination parts, the optical navigation sensor is able to measure the vehicle's distance even in poor lighting conditions unless the sensor moves on mirrors, glass, or a glossy surface.

The optical navigation sensor can be used as an odometer and does not suffer from slippage, which causes a serious problem in encoder-based odometry. Fig. 1 shows two parts of the optical navigation sensor, and more specific information is described in [10].

B. Inertial Measurement Unit (IMU)

An IMU measures velocity, orientation, and gravitational forces, using a combination of accelerometers and gyroscopes. By the aid of MEMS technology, it is easy to produce a small, low-cost MEMS IMU. In this study, we use an XSens MTi IMU in Fig. 2 which has a sensing range of 300deg/s (angular velocity) and 2g (acceleration) [11]. However, the acceleration output includes biased and random noises that change with the elapse of time, as shown in Fig. 3 . Moreover, acceleration values should be integrated to calculate the vehicle's position. Finally, the error accumulation of the position by noise is exacerbated. Therefore, we use only the angular velocity from the IMU output in the proposed algorithm.

C. Global Positioning System (GPS)

The GPS is a satellite navigation system that provides location and time information. It is operated by United States and is available to anyone who has a GPS receiver. The location data that are computed by the received data from the satellites contain some errors due to the following inherent limitations:

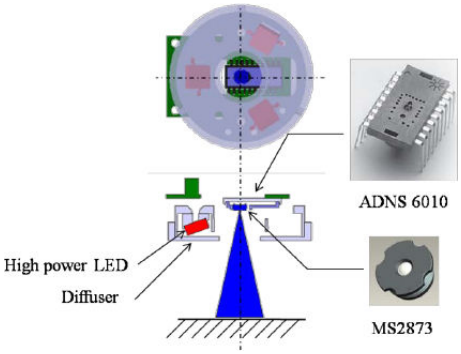

(a) Configuration

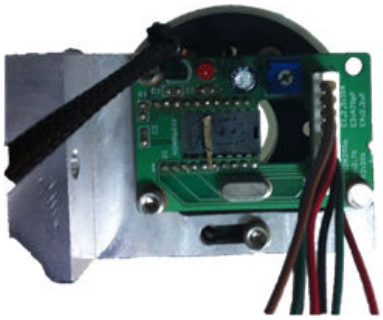

(b) Actual picture

Fig. 1. Description of optical navigation sensor

Fig. 2. Inertial Measurement Unit(IMU), Xsens MTi

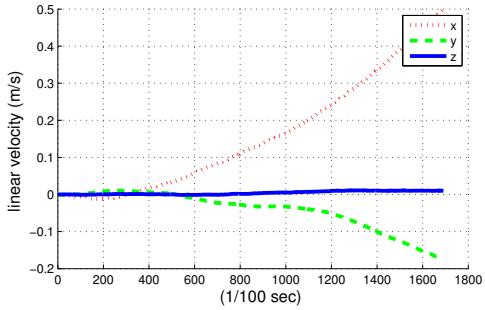

Fig. 3. Linear velocity measurement from Xsens MTi when robot stops. The linear velocity value is calculated by integration of linear acceleration, and biased drift was calibrated.

atmospheric effects, multipath effects, ephemeris and clock errors [12] [13].

To enhance localization accuracy, Differential Global Positioning System (DGPS) is used in our algorithm. DGPS has three different cases of implementation: Standard Real Time Kinematic (RTK), Moving Base, and Heading. In this paper, we used the standard RTK method [14] that is provided by the Ashtech DG14 GPS receiver [14]. The standard RTK system needs a fixed base station whose position is accurately known. The mobile robot, a rover, moves around the base station. The base station continuously sends correction data to the rover and the real-time position of the rover is calculated from the received data and the correction data. Fig. 4 shows this standard RTK scheme. When DGPS mode is activated, the rover can estimate its position with very small uncertainty (less than 2 3m). Nonetheless, DGPS mode needs high quality communication between a rover and a base station. If there is any communication interruption, DGPS mode stops operating.

In the proposed localization algorithm, both Single GPS mode and DGPS mode are used for correcting the mobile robot's position estimated by the optical navigation sensor and IMU.

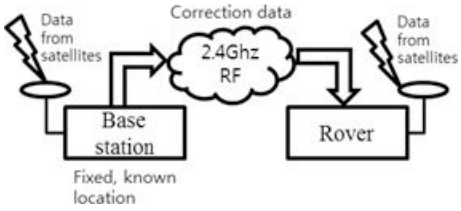

Fig. 4. Configuration of Stnadard Real Time Kinematics(RTK) GPS

III. Localization Algorithm with Optical Navigation Sensor, IMU and GPS

In this section, a novel outdoor localization algorithm is proposed. The algorithm is devised for an outdoor mobile robot moving around an urban area. The core algorithm is based on an Extended Kalman Filter (EKF), and environment information is acquired from a newly developed optical navigation sensor, IMU, and GPS. The optical navigation sensor provides transverse distance in the robot's x-axis, ρ, and IMU gives the angular velocity, ω, for state prediction. Absolute position information from GPS is used for the update step of the EKF.

A. Augmented Robot State

The optical navigation sensor needs a scale parameter to convert the sensor output value into a real distance value. The scale parameter is slightly changed depending on the ground condition or the texture of the surface. By calibrating the parameter autonomously, it is possible to estimate the robot pose more accurately. For autonomous calibration, a calibration parameter α is introduced. The calibration parameter α is a random variable modeled by a Gaussian distribution, and its variance slightly increases with the elapse of time by adding a constant random variable whose mean is zero and variance is σ_α as shown in (1).

$$\alpha_{k+1} = \alpha_k + \mathcal{N}(0, \sigma_\alpha) \tag{1}$$

The calibration parameter is added to the general robot state (x_k, y_k, θ_k) and simultaneously estimated by a localization algorithm [15]. The augmented state at the k_{th} step is represented by $\mathbf{x}_k$ as (2).

$$\mathbf{x}_k = [x_k \quad y_k \quad \theta_k \quad \alpha_k]^{\mathrm{T}} \tag{2}$$

B. Prediction Step

Prediction of the robot state is based on the transverse distance, ρ, acquired from optical navigation sensor and angular velocity, ω, acquired from the IMU. They are represented by the vector $\mathbf{u}_k$, as shown in (3).

$$\mathbf{u}_k = [\rho_k \quad \omega_k]^{\mathrm{T}} \tag{3}$$

Based on $\mathbf{u}_k$, mean prediction of robot state is conducted by (4).

$$\begin{aligned} \mathbf{x}_{k+1}^{-} &= f(\mathbf{x}_k, \mathbf{u}_k) \\ \begin{bmatrix} x_{k+1} \\ y_{k+1} \\ \theta_{k+1} \\ \alpha_{k+1} \end{bmatrix} &= \begin{bmatrix} x_k + \alpha_k \rho_k \cos(\Phi_k) \\ y_k + \alpha_k \rho_k \sin(\Phi_k) \\ \theta_k + \omega_k \Delta t \\ \alpha_k \end{bmatrix} \\ \text{where} \qquad \Phi_k &= \theta_k + \frac{1}{2}\omega_k \Delta t \end{aligned} \tag{4}$$

f is a prediction function for the robot state. $\mathbf{x}^{-}$ is the predicted mean before update, and Δt is the duration of prediction. Continuously, prediction of the covariance is performed by (5)

$$\begin{aligned} P_{k+1}^{-} &= J_x P_k J_x^{\mathrm{T}} + J_u Q_k J_u^{\mathrm{T}} + \sigma_\alpha^2 \zeta \zeta' \\ \text{where} \quad J_x &= \frac{\partial f}{\partial \mathbf{x}_k}, \quad J_u = \frac{\partial f}{\partial \mathbf{u}_k} \\ \zeta &= [0 \quad 0 \quad 0 \quad 1]^{\mathrm{T}} \end{aligned} \tag{5}$$

P^{-} is the predicted covariance matrix before the update, and P is the covariance after the update. J_x, J_u are Jacobian matrixes with regard to $\mathbf{x}, \mathbf{u}$ respectively. The last term of (5) is for adding noise to the calibration parameter α to realize the assumption of (1).

C. Update Step

In the update step of the EKF localization algorithm, GPS information is used as a measurement. GPS provides one of the most powerful tools available in outdoor environments because it gives absolute position information of a mobile robot, not relative information. The proposed algorithm uses two different GPS modes, as stated in the previous section, single GPS mode (GPS) and Differential GPS (DGPS) mode.

The single GPS mode utilizes only signals from satellites, and DGPS mode is operated by an additional GPS station. Single GPS mode is available in most outdoor environments, but the accuracy is not high due to reflection and blockage of the satellite signal and an insufficient number of satellites. In contrast, DGPS mode provides more accurate position of the vehicle, but its available area is quite limited due to communication problems. If the vehicle is out of the communication range or an obstacle blocks the signal from a GPS base station, communication fails and DGPS mode is unavailable.

In this paper, a novel update procedure is suggested with consideration of the characteristics of the optical navigation sensor, IMU, and two GPS modes. The update step follows (6) and (7).

$$\mathbf{x}_k = \mathbf{x}_k^{-} + K_k(\mathbf{z}_k - \hat{\mathbf{z}}_k) \tag{6}$$

$$P_k = [I - K_k H_k] P_k^{-} \tag{7}$$

Where

$$K_k = P_k^{-} H_k^{\mathrm{T}} \Psi_k^{-1} \tag{8}$$

$$\Psi_k = H_k P_k^{-} H_k^{\mathrm{T}} + R_k \tag{9}$$

$$\mathbf{z}_k = [x_{h_k} \quad y_{h_k} \quad \tan^{-1}\left(\frac{y_{h_k} - y_{h_{k-1}}}{x_{h_k} - x_{h_{k-1}}}\right)]^{\mathrm{T}} \tag{10}$$

$$\hat{\mathbf{z}}_k = h(\mathbf{x}_k) = [x_k \quad y_k \quad \theta_k]^{\mathrm{T}} \tag{11}$$

$$H_k = \frac{\partial h(\mathbf{x}_k)}{\partial \mathbf{x}_k} = \begin{bmatrix} 1 & 0 & 0 & 0 \\ 0 & 1 & 0 & 0 \\ 0 & 0 & 1 & 0 \end{bmatrix} \tag{12}$$

$$R_k = \begin{bmatrix} \sigma_{gps}^2 & 0 & 0 \\ 0 & \sigma_{gps}^2 & 0 \\ 0 & 0 & (\sigma_\theta(\sum |\omega| + \kappa_\omega)/(\sum \rho + \kappa_\rho))^2 \end{bmatrix} \tag{13}$$

K of (8) is Kalman gain, Ψ of (9) is an innovation matrix, $\mathbf{z}$ of (10) is measurement from GPS. The heading angle is calculated from the difference between previous and current GPS values. $\hat{\mathbf{z}}$ of (11) is the estimated measurement. H of (12) is the Jacobian of h. R of (13) is a measurement covariance matrix. σ_{gps} and σ_θ is alternatively selected depending on the GPS mode: single GPS or DGPS. $\sum |\omega|$ and $\sum \rho$ are the sum of $|\omega|$ and sum of ρ acquired from the previous to current GPS measurement. κ_ω and κ_ρ are small constants to prevent the variance of the heading angle measurement from becoming zero or an infinite value.

The remarkable point in the update step is (10) and (13). GPS provides only the vehicle's absolute position, namely x and y, but it does not give heading angle information. Nevertheless, update of the heading angle is very important to prevent uncertainty of the heading angle from divergence.

The most intuitive way of determining the vehicle's heading angle is to take advantage of the arc-tangent value between two GPS positions, as shown in (10). However, determining covariance is not a simple task. A robot does not travel straight all the time and sometimes moves slightly less than the GPS uncertainty. Considering these factors, covariance of the heading angle measurement is built as shown in (13). As the robot moves farther without turning, its covariance becomes smaller, and its scale is determined by parameters.

IV. Experiment

For verification of the proposed algorithm, an experiment is performed. The experiment is conducted with an outdoor mobile robot on the KIST campus, and the mobile robot path is organized to show the robustness of the algorithm effectively.

A. Hardware description

The outdoor mobile robot used for the experiment has the following specifications and Fig. 5 shows a photograph of the robot. The mobile robot is a skid-steering vehicle and is

Fig. 5. Unmanned ground vehicle which is equipped with newly developed optical navigation sensor, Xsens MTi IMU, Ashtech GPS and Maxon EC Motors. It is a skid-steering vehicle and operated by a laptop.

equipped with an optical navigation sensor, Xsens MTi IMU, and Ashtech DG14 GPS for localization. All wheels are driven by Maxon 250W EC motors. The vehicle's operating program is written in C++ language under an Intel Atom 1.6Ghz processor laptop PC with Windows XP. Additionally, a TI LM3S8962 microcontroller board is used to collect optical and IMU sensor data at 100Hz. The collected data are sent to a laptop PC every 10ms. The GPS position outputs position data that are enhanced with a Real-Time Kinematic (RTK) algorithm at 5Hz. We used the standard RTK algorithm supported by the DG14 receiver, which has a static base station. With this mobile robot, we conducted an experiment to demonstrate the performance of the proposed localization algorithm.

B. Experiment Result

The experiment was performed with the above robot on the campus of KIST. In the experiment the robot continuously moves on grass and paved ground in the vicinity of many buildings. The experiment site represents a typical urban environment. Fig. 6 shows the robot's path and the experiment environment, and further details are provided below.

First, the robot started moving on point A in Fig. 6(a) which exists on the grass as shown in Fig. 6(b). Then, across the boarder (Point C, Fig. 6(d)), the robot entered paved ground (refer to Fig. 6(c)) where a large building (Area E of Fig. 6(a)) is located. Next, the robot returned from the paved road, and re-entered the grass area through a border (Point D). Lastly, the robot moved with complex and sharp turning and finally arrived at Point B.

As shown in Fig. 6(a), the GPS signal was frequently interrupted. Thus, GPS mode frequently alters between DGPS mode (marked by a green '*') and Single GPS mode (marked by a red 'x'). Particularly when the robot passed beside a tall building (Path C-D), the quality of GPS was extremely low. The reason is that the number of available satellites was very small and, even worse, the remaining signals were very noisy due to reflection by buildings.

In addition to the GPS trouble, the uneven ground surface conditions also made localization more difficult. The surface of the grass is rough, and this leads to wheel revolution in the air and slippage. Moreover, in the transition phase between the paved ground and the grass, the robot received a strong shock and drifted abruptly.

Despite the above severe conditions, the localization algorithm showed stable performance as shown in Fig. 6(a). When GPS information was uncertain, although the covariance became larger, the estimated path did not seriously deviate from the actual path. When DGPS mode became available again, the algorithm rapidly recovered its uncertainty. Furthermore, the mobile robot was consistently able to estimate its path even during continual slippage and disturbances from surface transition.

V. Conclusion

In this paper, we suggested a novel localization algorithm with a newly developed optical navigation sensor, IMU, and GPS. Its performance was verified by an experiment in an urban environment. The experiment results show that the proposed localization algorithm is able to maintain stable performance even under very severe conditions: GPS signal interruption and uneven ground surface.

From the analysis of the results, it is found that the primary factor for these desirable results is the advantage of the optical navigation sensor. In outdoor navigation, unpredictable and various external dynamical effects that make mobile robot localization difficult are inevitable. The greatest advantage of our newly developed optical navigation sensor is that it is invariant to such external influences. Although the mobile robot is subjected to various and sudden external effects, the optical navigation sensor could successfully estimate the robot pose.

Additionally, correction of the heading angle from GPS information was considered to be an important issue in developing the localization algorithm. In particular, covariance of the heading angle measurement was built after long consideration and several trials, because both the IMU and optical navigation sensor information should be considered concurrently. Finally, the covariance of the heading angle measurement was built as (13), and as shown in the experiment results, the mobile robot's heading is successfully estimated.

Experiment results show the potential of the optical navigation sensor for outdoor navigation. As future study, sensor

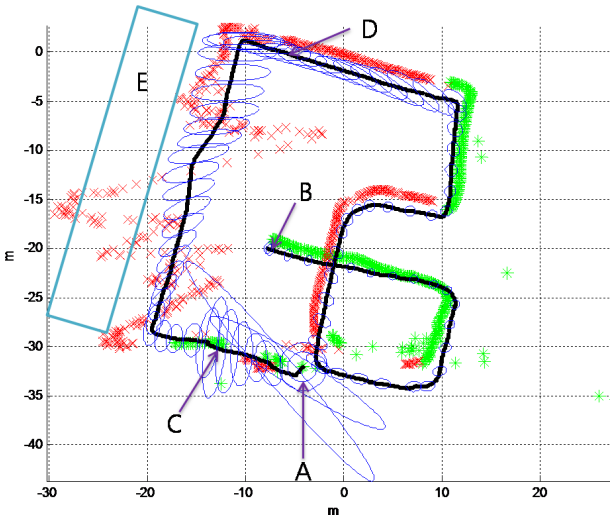

(a) Localization result; Red: Single GPS data, Green: DGPS(Differential GPS) data, Black: estimated robot pose, Blue eclipse: size of covariance(scaled), A: start point, B: end point, C,D: border of the grass, E: a tall building, fixed GPS base stands on the top of this building

(b) The grass (A-C, D-B)

(c) The paved ground (C-D)

(d) Border of the grass (C,D)

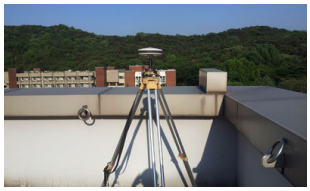

(e) Fixed GPS base

Fig. 6. Description of experiment environment and result analysis

fusion with other sensors such as a magnetic compass or LRF would be an interesting subject.

VI. ACKNOWLEDGMENTS

This work was supported by the Dual-Use Technology program of Defense Acquisition Program Administrator/Dual Use Technology Center and Ministry of Knowledge Economy/Institute for Information Technology Advancement of Republic of Korea. [06-DU-LC-01, Development of Multi-Purpose Dog-Horse based on the Network]

REFERENCES

[1] S. Cooper and D. H. Whyte, "A Kalman filter model for GPS navigation of land vehicles," in *IEEE/RSJ/GI International Conference on Intelligent Robots and Systems*, pp. 157–163, 1994.

[2] A. Georgiev and P. K. Allen, "Localization methods for a mobile robot in urban environments," *IEEE Transactions on Robotics*, 2004.

[3] J. ichi Meguro, T. Hashizume, J. ichi Takiguchi, and R. Kurosaki, "Development of an autonomous mobile surveillance system using a network-based rtk-gps," in *International Conference on Robotics and Automation*, pp. 3096–3101, 2005.

[4] L. Ojeda and J. Borenstein, "Methods for the reduction of odometry errors in over-constrained mobile robots," *Auton. Robots*, 2004.

[5] G. Anousaki and K. J. Kyriakopoulos, "A dead-reckoning scheme for skid-steered vehicles in outdoor environments," in *International Conference on Robotics and Automation*, pp. 580–585, 2004.

[6] S. Panzieri, F. Pascucci, and G. Ulivi, "An outdoor navigation system using gps and inertial platform," *IEEE/ASME Trans. on Mechatronics*, 2002.

[7] P. Stone and P. Stone, "Simultaneous calibration of action and sensor models on a mobile robot," in *International Conference on Robotics and Automation*, 2004.

[8] A. Mandow, J. Martínez, J. Morales, J.-L. Blanco, A. García-Cerezo, and J. González-Jiménez, "Experimental kinematics for wheeled skid-steer mobile robots," in *Proc. of IEEE/RSJ Int. Conf. on Intelligent Robots and Systems*, 2007.

[9] K. Ohno, T. Tsubouchi, and S. Yuta, "Outdoor map building based on odometry and rtk-gps positioning fusion," in *International Conference on Robotics and Automation*, pp. 684–690, 2004.

[10] D. Hyun, H. Yang, H. Park, and H. Kim, "Dead-reckoning sensor system and tracking algorithm for 3-d pipeline mapping," *IEEE/ASME Trans. on Mechatronics*, 2010.

[11] "http://www.xsens.com/en/general/mti."

[12] "http://pnt.gov/public/docs/2008/spsps2008.pdf."

[13] B. W. Parkinson and J. J. Spiker, *Global Positioning System: Theory and Applications (Volume One)*. Progress in Astronautics and Aeronautics, 1996.

[14] "www.ashtech.com/dg-14-2663.kjsp."

[15] Y. Yun, B. Park, and W. K. Chung, "Odometry calibration using home positioning function for mobile robot," in *International Conference on Robotics and Automation*, pp. 2116–2121, 2008.